

# A new molecular precursor for magnesia–silica materials

Joshua W. Kriesel<sup>a,b</sup> and T. Don Tilley<sup>\*a,b</sup>

<sup>a</sup>Department of Chemistry, University of California, Berkeley, Berkeley, California, 94720-1460, USA

<sup>b</sup>The Chemical Sciences Division, Lawrence Berkeley National Laboratory, 1 Cyclotron Road, Berkeley, California, 94720, USA

Received 25th September 2000, Accepted 5th December 2000  
First published as an Advance Article on the web 5th March 2001

The new molecular precursor  $\text{Mg}[\text{OSi}(\text{O}^t\text{Bu})_3]_2$  was synthesized in high yield from  $\text{Mg}(\text{Bu})_2$  and  $\text{HOSi}(\text{O}^t\text{Bu})_3$ . Thermolytic decomposition of this precursor in toluene solution leads to a magnesia–silica monolith. The monolith can be processed to isolate xerogels or aerogels with surface areas of 245 and  $640 \text{ m}^2 \text{ g}^{-1}$ , respectively. The  $\text{MgO} \cdot 2\text{SiO}_2$  materials are very acidic, as determined by ammonia temperature programmed desorption (TPD). Additionally,  $\text{CO}_2$  TPD revealed that these materials have a very low basic site density. The TPD results can be explained by a very high dispersion of  $\text{MgO}$  in an  $\text{SiO}_2$  matrix, and are consistent with predictions based on charge balancing in binary oxides.

## Introduction

Recently, there has been increasing interest in the discovery of advanced materials with complex stoichiometries and novel architectures. These materials have attracted significant attention due to their potential applications as, for example, catalyst supports, refractory materials and molecular sieves. Accordingly, a major challenge in materials science is the development of synthetic protocols that allow precise control of solid-state structure at the atomic level.<sup>1</sup> One approach to materials with well-defined stoichiometries involves the use of molecular precursors that contain all the elements for the desired material in a single source.<sup>2</sup>

We have focused efforts on developing alternative routes to the sol–gel method, for the synthesis of metal oxides and composite materials.<sup>3</sup> Sol–gel protocols involve the hydrolysis of metal alkoxides, which, following condensation of the hydrolyzed species, yield metal oxide materials that can be processed into monoliths, fibers, thin-films and porous gels. Although this method has found wide application, it has two major limitations. Firstly, sol–gel chemistry typically takes place in polar solvents (*e.g.* water or alcohol), and therefore the isolated gels undergo severe pore collapse upon desiccation of the “wet” gel.<sup>4</sup> Secondly, in order to access mixed-element oxides *via* the sol–gel method, multiple ( $\geq 2$ ) metal alkoxide precursors are usually employed. This can lead to heterogeneous mixtures of metal oxide materials ( $\text{M–O–M}$  and  $\text{M'–O–M'}$ ), due to the fact that different metal alkoxide species typically hydrolyze at different rates.<sup>5</sup> We have accessed homogeneous mixed-element oxides by way of the thermolytic decomposition of single-source precursors containing  $-\text{OSi}(\text{O}^t\text{Bu})_3$  and  $-\text{O}(\text{O})\text{P}(\text{O}^t\text{Bu})_2$  groups. These oxygen-rich, mixed-element compounds eliminate isobutylene and water at low temperatures ( $90\text{--}150^\circ\text{C}$ ) in the solid-state or in solution. In particular, this thermolytic molecular precursor route has been shown to be effective for producing highly dispersed metal oxide–silica and metal phosphate materials.<sup>3</sup>

A primary goal of synthetic efforts in catalysis research is the control of surface acid–base properties. Solid acid and base catalysts have received significant attention due, for example, to their ability to dehydrate alcohols and isomerize olefins.<sup>6</sup>

Alkaline earth oxides are known to have highly basic properties, and  $\text{MgO}$  has been targeted as a particularly useful basic metal oxide catalyst support.<sup>6,7</sup>

Binary alkaline earth oxide–silica materials may be used as either acidic or basic catalysts.<sup>6–10</sup> Lopez *et al.* prepared  $\text{MgO–SiO}_2$  materials *via* the cohydrolyses of silicon and magnesium alkoxides under both acidic and basic conditions.<sup>9a</sup> Results from this study indicated that basicity in the  $\text{MgO–SiO}_2$  system is related to the degree of segregation of magnesia in the material: that is, materials containing “magnesia islands” (*i.e.*, a heterogeneous system) are more basic. Simple charge-balancing arguments by Tanabe suggest that a homogeneous  $\text{MgO} \cdot 2\text{SiO}_2$  material (*i.e.*, containing  $\text{Mg–O–Si}$  bonds) would have a higher acid strength than either magnesia or silica.<sup>11</sup> Thus, there appears to be an inherent correlation between dispersity and the acid–base properties of magnesia–silica materials. To our knowledge, few attempts have been made to synthesize highly homogeneous  $\text{MgO–SiO}_2$  systems. Given this situation, it seemed that the thermolytic molecular precursor route to magnesia–silica materials might provide some control over acid–base properties, and perhaps produce materials with useful catalytic (acid–base) properties.

This report describes our efforts to prepare well-dispersed  $\text{MgO–SiO}_2$  materials from the single-source molecular precursor  $\text{Mg}[\text{OSi}(\text{O}^t\text{Bu})_3]_2$  (**1**). Thermolytic decomposition of **1** in toluene led to monolithic gels with the approximate composition  $\text{MgO} \cdot 2\text{SiO}_2$ . The “wet” gels were processed to form xerogels and aerogels, and their pore structures were characterized by  $\text{N}_2$  porosimetry. Additionally, we have determined certain acid–base properties for these new materials, which appear to provide information concerning their homogeneity.

## Results and discussion

The new magnesium siloxide  $\text{Mg}[\text{OSi}(\text{O}^t\text{Bu})_3]_2$  (**1**) was prepared by the reaction of dibutylmagnesium and the silanol in THF solution at room temperature (eqn. 1). This reaction is quantitative by NMR spectroscopy and the isolated yield was 83% following crystallization from pentane. Despite numerous attempts, we were unable to obtain single crystals of **1** suitable

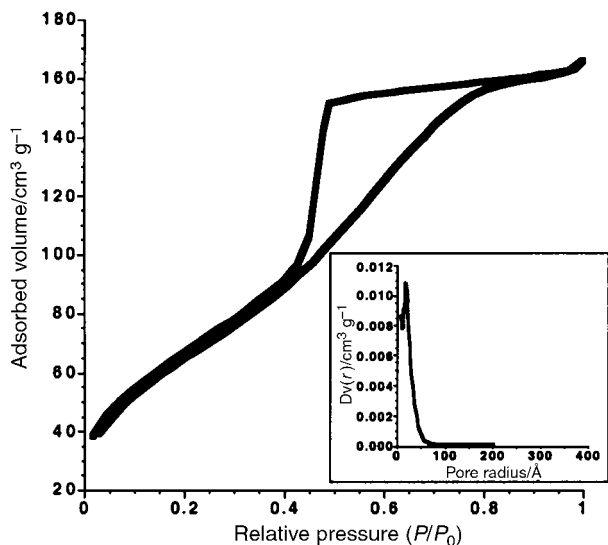
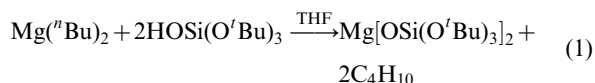


**Fig. 1** The N<sub>2</sub> isotherm for the xerogel made from **1** (MgO·2SiO<sub>2</sub>). The corresponding BJH pore size distribution, shown in the inset, was calculated from the adsorption branch of the isotherm.

for single crystal X-ray diffraction. Therefore, this compound was characterized by spectroscopic methods and combustion analysis. A solution molecular weight analysis of **1** demonstrated that the complex is monomeric in benzene solution. Given the great preference of magnesium for coordination number 4 (over 2), we assume that both siloxide ligands in **1** are bound in an η<sup>2</sup>-fashion, by coordination of a *tert*-butoxy oxygen atom to magnesium. This coordination mode has previously been observed in zirconium<sup>3h</sup> and zinc<sup>3g</sup> complexes. Compound **1** is extremely moisture sensitive, and hydrolyzes instantly in air. The moisture sensitivity of **1** complicated attempts to obtain a meaningful thermogravimetric analysis (TGA).



MgO·2SiO<sub>2</sub> xerogels were obtained by heating **1** in toluene solution in a sealed ampoule for 12 h at 185 °C. An opaque monolith, which became clear upon cooling of the reaction vessel, was obtained. During air-drying, the monolith shrank (by ca. 70%) and cracked into several pieces over 5 d. Elemental analysis of this material revealed a Mg : Si ratio of 1 : 2.3, which is close to that expected for MgO·2SiO<sub>2</sub>. Additionally, the as-isolated xerogel (no additional drying under vacuum) was found to possess a very low carbon content (0.77%).

After further drying of the xerogel under vacuum at 120 °C, N<sub>2</sub> porosimetry was performed (see Fig. 1 and Table 1). This analysis revealed that the nitrogen adsorption isotherm was type IV, which arises from capillary condensation inside a mesoporous solid. Additionally, the corresponding adsorption-desorption loop is reminiscent of type H2 hysteresis<sup>12</sup> (type E in the older literature<sup>13</sup>). This type of adsorption-desorption isotherm has been attributed to ink-bottle type pores,<sup>13</sup> although it is now recognized that this may be an

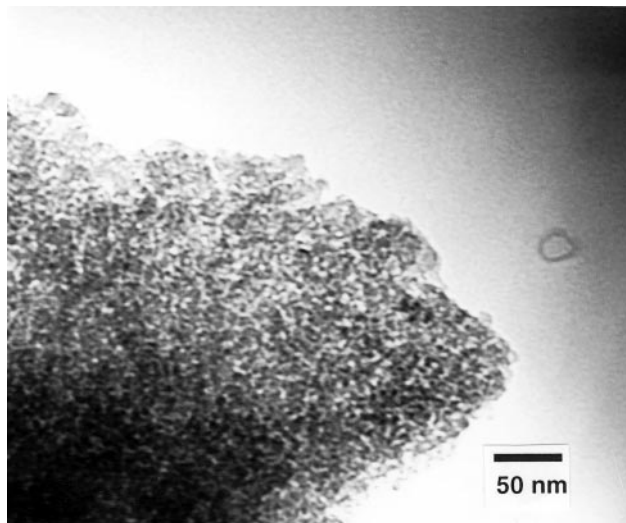


**Fig. 2** A TEM micrograph of the xerogel obtained from **1**.

oversimplification of the actual pore structure.<sup>12</sup> The BJH pore size distribution<sup>13</sup> for the xerogel derived from **1** was calculated from the adsorption branch of the isotherm and reveals a relatively narrow pore size distribution (Fig. 1) with a corresponding average pore radius of 17 Å. The BET surface area of this material was 245 m<sup>2</sup> g<sup>-1</sup>.

TEM micrographs of MgO·2SiO<sub>2</sub> (Fig. 2) reveal a xerogel composed of small primary particles (≤ 5 nm). The particle packing appears to have produced a fine texture, *i.e.* very little “textural porosity.” As determined by the TEM analysis, this well-defined mesoporosity is apparently a result of the packing of monodisperse particles in this material.

In order to obtain an MgO·2SiO<sub>2</sub> material with a higher surface area, the wet gel obtained from thermolysis of **1** in toluene was processed using supercritical CO<sub>2</sub> extraction. Thus, the wet gel monolith was placed in a critical point dryer, the solvent exchanged with liquid CO<sub>2</sub>, and subsequently the CO<sub>2</sub> was removed supercritically. The aerogel, which was analyzed as having an Mg : Si ratio of 1 : 2.3, was opaque and yellow in color, but transparent when viewed with a bright light.

The N<sub>2</sub> isotherm for the MgO·2SiO<sub>2</sub> aerogel (Fig. 3) corresponds to a large adsorbed volume at high relative pressure, and in this regard is similar to what has been observed for silica aerogels.<sup>14</sup> Additionally, the surface area and pore volume of this material (640 m<sup>2</sup> g<sup>-1</sup> and 3.58 cm<sup>3</sup> g<sup>-1</sup>, respectively) are significantly larger than corresponding values for the xerogel. Furthermore, the pore size distribution derived from the adsorption branch of the isotherm exhibits a maximum pore radius of 16 Å and is very broad. However, it is important to note that nitrogen adsorption-desorption porosimetry has been shown to be inaccurate for determining pore volumes and sizes in aerogels,<sup>15</sup> and therefore these data may be misleading. TEM micrographs of the aerogel derived from **1** reveal an open, fibrous network composed of small spherical grains loosely packed together (Fig. 4).

To investigate the thermal stability and crystallization behavior of the MgO·2SiO<sub>2</sub> gels, these materials were heated under oxygen and subsequently studied by powder X-ray

**Table 1** Nitrogen porosimetry data for the gels derived from **1**

Sample	BET surface area/m <sup>2</sup> g <sup>-1</sup>	Total pore volume/cm <sup>3</sup> g <sup>-1</sup>	Average pore radius/Å <sup>a</sup> (2 V/A)	Average pore radius/Å <sup>b</sup> (BJH)	Micropore area/m <sup>2</sup> g <sup>-1</sup>
X-MgO <sub>2</sub> ·2SiO <sub>2</sub> <sup>c</sup>	245	0.26	21	17	0
A-MgO <sub>2</sub> ·2SiO <sub>2</sub> <sup>d</sup>	640	3.58	112	16	0

<sup>a</sup>Average pore radii were calculated using 2(pore volume)/surface area. <sup>b</sup>The BJH average pore radii were determined from the global maximum of the adsorption pore size distribution. <sup>c</sup>Xerogel. <sup>d</sup>Aerogel.

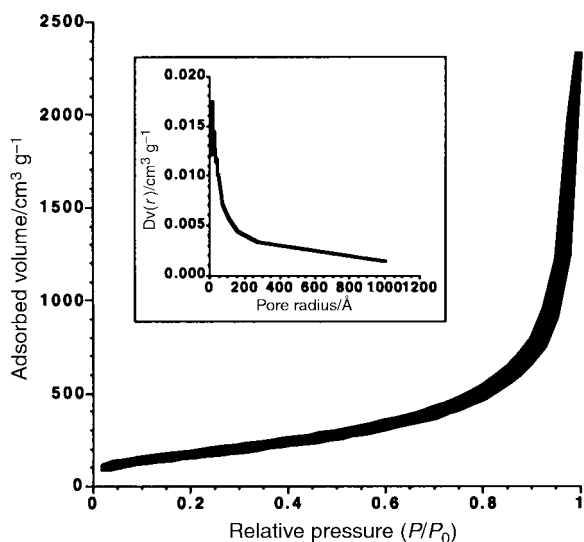


**Fig. 3** The  $N_2$  isotherm for the aerogel made from **1** ( $MgO \cdot 2SiO_2$ ). The corresponding BJH pore size distribution, shown in the inset, was calculated from the adsorption branch of the isotherm.

diffraction (XRD). As isolated, both the xerogel and the aerogel obtained from **1** were amorphous. After calcination to  $1200^\circ C$  under  $O_2$ , enstatite ( $MgSiO_3$ ) was observed by powder XRD.

Temperature programmed desorption (TPD) was performed on the magnesia–silica xerogel in order to obtain information on the acidity and basicity of these materials. In particular,  $NH_3$  TPD was first used to estimate the number of acid sites after pretreating the xerogel under flowing He at  $200^\circ C$  for 1 h. Subsequently,  $NH_3$  was passed over the material at room temperature and then thermal desorption was monitored by mass spectral analysis at a heating rate of  $10^\circ C \text{ min}^{-1}$  to  $800^\circ C$ . As shown in Fig. 5, the majority of the ammonia desorption occurs between 100 and  $500^\circ C$ . Using these data, the number of acid sites was estimated to be  $2.7 \text{ nm}^{-2}$ . This is higher than analogous values for magnesia–silica xerogels made by Lopez *et al.* using an acid-catalyzed sol–gel route, followed by sulfation ( $0.3\text{--}2.4 \text{ acid sites nm}^{-2}$ ).<sup>9a</sup>

A carbon dioxide TPD analysis was performed in order to quantify the basic site density on the  $MgO \cdot 2SiO_2$  xerogel. As shown in Fig. 6, the TPD thermogram reveals the presence of two distinct peaks. The peaks at *ca.* 80 and  $410^\circ C$  can be attributed to weak and strong basic sites, respectively. Using these data, the basic site distribution in the  $MgO \cdot 2SiO_2$  xerogel

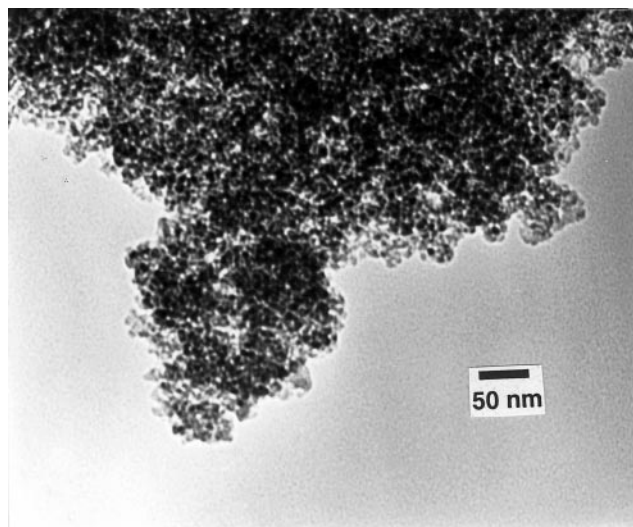


**Fig. 4** A TEM micrograph of the aerogel obtained from **1**.

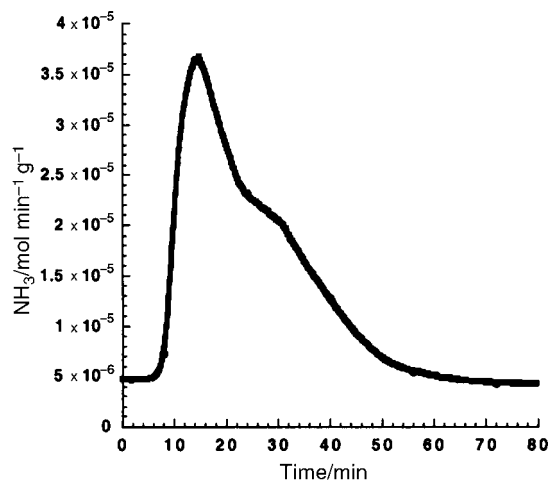


**Fig. 5** The  $NH_3$  temperature programmed desorption (TPD) thermogram for the xerogel obtained from **1**, for which the temperature was ramped from  $25$  to  $800^\circ C$  at a rate of  $10^\circ C \text{ min}^{-1}$ .

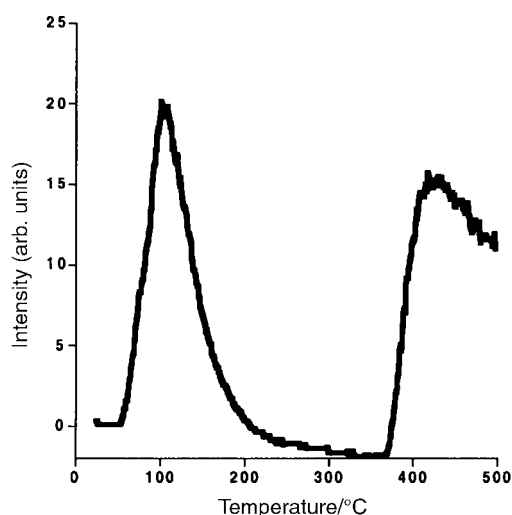


**Fig. 6** The  $CO_2$  temperature programmed desorption (TPD) thermogram for the xerogel obtained from **1**.

was determined to be  $23.3 \mu\text{mol g}^{-1}$  for the weak basic sites and  $26.5 \mu\text{mol g}^{-1}$  for the strong basic sites. In terms of a weak and strong basic site density, this corresponds to 0.06 and  $0.07 \text{ basic sites nm}^{-2}$ , respectively. Thus, the xerogel derived from **1** is in fact devoid of significant basicity. This may be due to the fact that the  $MgO$  is very well dispersed within the  $SiO_2$  matrix.

For magnesia–silica materials for which  $SiO_2$  is the major component, Tanabe has predicted the presence of significant acid strength using a model that features charge balancing in binary oxides.<sup>11</sup> Moreover, Tanabe predicted, and subsequently confirmed experimentally, that the number of acid sites of the mixed oxide is greater than the sum of those of magnesia and silica. Thus, the relatively high number of acid sites for the xerogel derived from **1** (as determined by  $NH_3$  TPD) is consistent with the theoretical and experimental results of Tanabe, assuming a high level of dispersity.

Further, our findings seem consistent with the work of Lopez *et al.*, who have examined magnesia–silica materials with apparently different homogeneities. The cohydrolysis of magnesium diethoxide and tetraethoxysilane under basic conditions appeared to give phase-segregated magnesia, probably due to the relatively slow base-catalyzed hydrolysis of  $Si(OEt)_4$  relative to  $Mg(OEt)_4$ . Such samples displayed a

higher basicity than samples prepared under acidic conditions, which were believed to be more highly dispersed. Therefore, given the acidic (and nonbasic) properties of the MgO–SiO<sub>2</sub> xerogel derived from **1**, this material appears to be highly homogeneous with a high concentration of Mg–O–Si hetero-linkages.

## Conclusion

The thermolytic molecular precursor route to magnesia–silica materials, using the new precursor Mg[OSi(O<sup>t</sup>Bu)<sub>3</sub>]<sub>2</sub> (**1**), has been described. The transformation of **1** in toluene solution provides xerogels and aerogels with high surface areas. These materials remain amorphous by XRD to 1100 °C, after which the crystallization of enstatite (MgSiO<sub>3</sub>) occurs. Ammonia TPD experiments revealed that the MgO·2SiO<sub>2</sub> xerogel is quite acidic (in terms of the Brønsted acid site density), which is consistent with the predictions based on charge balancing in binary oxides. Further, CO<sub>2</sub> TPD analysis suggests that these materials have a very low basic site density. This is most readily explained by a very high dispersion of MgO in an SiO<sub>2</sub> matrix, based on the predictions of Tanabe<sup>6</sup> and on the results of Lopez.<sup>9a</sup> These results therefore indicate that the thermolytic transformation of **1** in solution represents a useful method for the synthesis of materials with highly dispersed magnesia–silica phases. We intend to pursue this theme with further studies on materials derived from **1** and by investigation of **1** as a catalyst support.

## Experimental

### General

All reactions were performed under an inert dinitrogen atmosphere using standard Schlenk techniques. Tetrahydrofuran and pentane were distilled from purple sodium–benzophenone ketyl, and toluene was distilled from potassium. Dibutylmagnesium was obtained from Aldrich as a 1.0 M solution in heptane and stored under a dinitrogen atmosphere. Elemental analyses were performed by Mikroanalytisches Labor Pascher and for the Mg and Si analyses, V<sub>2</sub>O<sub>5</sub> was used as a catalyst. TEM micrographs were taken on a JEOL 200cx at 200 kV by depositing a pentane suspension of the finely ground gel on a “Type A” carbon coated Cu grid obtained from Ted Pella Inc. The N<sub>2</sub> porosimetry data were collected on a Micromeritics ASAP 2010 instrument using either a 60 or 80 point analysis, after degassing for a least 24 h at 120 °C. The infrared spectra were recorded on a Perkin-Elmer 1330 infrared spectrometer as Nujol mulls on KBr plates and all absorptions are reported in cm<sup>-1</sup>. Thermal analyses were performed on a TA instruments SDT 2960 Simultaneous DTA-TGA. The solution molecular weight was obtained by the Singer method. Powder X-ray diffraction was performed on a Siemens D5000 diffractometer. The tris(*tert*-butoxy)silanol was prepared as described elsewhere.<sup>16</sup>

Ammonia temperature programmed desorption (TPD) was performed at U.C. Berkeley in the laboratory of Professor Enrique Iglesia by first treating 0.31 g of the MgO·2SiO<sub>2</sub> xerogel at 200 °C in He for 1 h (1.67 cm<sup>3</sup> s<sup>-1</sup>). The NH<sub>3</sub> was then adsorbed by exposing treated samples to a stream containing 0.93% in He (100 cm<sup>3</sup> min<sup>-1</sup>) for 1 h at 25 °C. Ammonia was then desorbed in He flow (50 cm<sup>3</sup> min<sup>-1</sup>) by increasing the temperature at 10 °C min<sup>-1</sup> to 800 °C and measuring the intensity at 16 amu by mass spectrometry (Leybold-Inficon Transpector H200M). The acid site density was then calculated by integration of the entire intensity (mol min<sup>-1</sup> g<sup>-1</sup>) vs. time (min) plot.

Carbon dioxide TPD was performed by Quantachrome corporation. The two peaks observed in the TPD thermogram were quantified by comparison to a calibration thermogram

obtained by injecting known amounts of CO<sub>2</sub> into the system. Before CO<sub>2</sub> adsorption, the sample was pretreated in an He flow at 500 °C. After admitting CO<sub>2</sub>, the temperature was increased at a rate of 10 °C min<sup>-1</sup>. The basic site density was calculated by integration of the peaks, assuming standard temperature and pressure.

### Mg[OSi(O<sup>t</sup>Bu)<sub>3</sub>]<sub>2</sub> (**1**)

To a 100 cm<sup>3</sup> Schlenk flask containing 6.07 g (0.0230 mol, 2.02 equiv.) and 30 cm<sup>3</sup> of THF at 0 °C was added 11.4 cm<sup>3</sup> (0.0114 mol) of dibutylmagnesium *via* syringe. Bubbling subsided after *ca.* 1 min, and the clear solution was stirred for an additional 1 h at 0 °C, and then overnight at room temperature. After removal of the solvent *in vacuo*, the powdery white residue was extracted with pentane (20 cm<sup>3</sup>) and the resulting extract was concentrated and cooled to –40 °C. The resulting transparent crystals turned opaque upon isolation. Two crops of crystals were obtained, affording 5.18 g of **1** in 82.7% yield. Anal. calcd for C<sub>24</sub>H<sub>54</sub>O<sub>8</sub>Si<sub>2</sub>Mg: C, 52.30; H, 9.87. Found: C, 52.49; H, 10.23%. <sup>1</sup>H NMR (benzene-*d*<sub>6</sub>): δ 1.54. <sup>13</sup>C NMR (benzene-*d*<sub>6</sub>): δ 32.34 (CMe<sub>3</sub>), 25.38 (CMe<sub>3</sub>). IR: 2964, 2927, 1384, 1242, 1197, 1056, 974, 820, 698. Molecular weight in benzene: 545 g mol<sup>-1</sup>. Calculated for the monomer: 551 g mol<sup>-1</sup>.

### Xerogel obtained from **1**

A toluene solution (3.0 cm<sup>3</sup>) of compound **1** (0.50 g) was sealed under vacuum in an ampoule after 4 freeze–pump–thaw cycles. The ampoule was then placed in an oven preheated to 190 °C for 16 h, after which time a clear, colorless monolithic gel was obtained. The solid wet gel was removed from the ampoule and allowed to air-dry for 5 d, after which time the monolith cracked into several pieces and shrank by *ca.* 70%. The elemental analysis was done without calcination of the xerogel. Anal. calcd for O<sub>5</sub>Si<sub>2</sub>Mg: Si, 35.00; Mg, 15.15. Found: Si, 31.4; Mg, 13.6%. IR: 3421 (br), 1650, 1030 (br). Anal. found for C and H: C, 0.77; H, 3.11%.

### Aerogel obtained from **1**

A procedure identical to that employed for the synthesis of the xerogel was used, except that after obtaining the wet gel, solvent processing was performed using a jumbo SPI critical point dryer. In particular, the monolith was placed in the critical point dryer and the solvent was exchanged with flowing liquid CO<sub>2</sub> over 3 h. The monolith was maintained in the apparatus (fully submerged in liquid CO<sub>2</sub>) overnight. Subsequently, an additional 1–2 h of CO<sub>2</sub> purging was conducted, after which time the temperature of the critical point dryer was raised to 45 °C and the pressure rose to *ca.* 1400 psi. After maintaining the vessel under these conditions for several minutes, it was slowly vented over 20 min. The monolith changed from clear to opaque and yellow in color. Anal. calcd for O<sub>5</sub>Si<sub>2</sub>Mg: Si, 35.00; Mg, 15.15. Found: Si, 28.6; Mg, 12.2%. IR: 3413 (br), 1641, 1043 (br).

## Acknowledgements

This work was supported by the Director, Office of Basic Energy Sciences, Chemical Sciences Division, of the US Department of Energy under Contract No. DE-AC03-76SF00098. We also thank Professor Enrique Iglesia for use of his equipment for TPD studies.

## References

- (a) *Ultrastructure Processing of Ceramics, Glasses, and Composites*, ed. L. L. Hench and D. R. Ulrich, Wiley, New York, 1984; (b) *Ultrastructure Processing of Advanced Materials*, ed.

- D. R. Uhlmann and D. R. Ulrich, Wiley, New York, 1992; (c) *Better Ceramics Through Chemistry VI*, ed. A. K. Cheetham, C. J. Brinker, M. L. Mecartney and C. Sanchez, *Materials Research Society Symposium Proceedings*, Vol. 360, Materials Research Society, Pittsburgh, 1994, and previous volumes in this series; (d) *Materials Chemistry—An Emerging Discipline*, ed. L. V. Interrante, L. A. Casper and A. B. Ellis, *Advances in Chemistry Series 245*, American Chemical Society, Washington, DC, 1992; (e) *Inorganic Materials*, ed. D. W. Bruce and D. O'Hare, Wiley, New York, 1992; (f) A. Stein, S. W. Keller and T. E. Mallouk, *Science*, 1993, **259**, 1558.
- 2 Selected references on the single-source precursor approach: (a) A. H. Cowley and R. A. Jones, *Angew. Chem., Int. Ed. Engl.*, 1989, **28**, 1208; (b) A. G. Williams and L. V. Interrante, in *Better Ceramics Through Chemistry*, ed. C. J. Brinker, D. E. Clark and D. R. Ulrich, *Materials Research Society Symposia Proceedings*, Vol. 32, North-Holland, New York, 1984, p. 152; (c) A. W. Apblett, A. C. Warren and A. R. Barron, *Chem. Mater.*, 1992, **4**, 167; (d) F. Chaput, A. Lecomte, A. Dauger and J. P. Boilot, *Chem. Mater.*, 1989, **1**, 199; (e) D. M. Hoffman, *Polyhedron*, 1994, **13**, 1169; (f) R. C. Mehrotra, *J. Non-Cryst. Solids*, 1990, **121**, 1; (g) L. G. Hubert-Pfalzgraf, *New. J. Chem.*, 1987, **11**, 663; (h) D. C. Bradley, *Polyhedron*, 1994, **13**, 1111; (i) C. D. Chandler, C. Roger and M. J. Hampden-Smith, *Chem. Rev.*, 1993, **93**, 1205.
- 3 (a) K. W. Terry and T. D. Tilley, *Chem. Mater.*, 1991, **3**, 1001; (b) K. W. Terry, P. K. Gantzel and T. D. Tilley, *Chem. Mater.*, 1992, **4**, 1290; (c) K. W. Terry, P. K. Gantzel and T. D. Tilley, *Inorg. Chem.*, 1993, **32**, 5402; (d) K. W. Terry, C. G. Lugmair, P. K. Gantzel and T. D. Tilley, *Chem. Mater.*, 1996, **8**, 274; (e) C. G. Lugmair, T. D. Tilley and A. L. Rheingold, *Chem. Mater.*, 1997, **9**, 339; (f) K. Su and T. D. Tilley, *Chem. Mater.*, 1997, **9**, 588; (g) K. Su, T. D. Tilley and M. J. Sailor, *J. Am. Chem. Soc.*, 1996, **118**, 3459; (h) K. W. Terry, C. G. Lugmair and T. D. Tilley, *J. Am. Chem. Soc.*, 1997, **119**, 9745.
- 4 C. J. Brinker and G. W. Scherer, *Sol-Gel Science: The Physics and Chemistry of Sol-Gel Processing*, Academic Press, San Diego, 1990.
- 5 (a) *Sol-Gel Technology for Thin Films, Fibers, Preforms, Electronics, and Specialty Shapes*, ed. L. C. Klein, Noyes, Park Ridge, NJ, 1988; (b) R. J. P. Corriu and D. Leclercq, *Angew. Chem., Int. Ed. Engl.*, 1996, **35**, 1421; (c) M. Guglielmi and G. Carturan, *J. Non-Cryst. Solids*, 1988, **100**, 16; (d) C. J. Brinker, *J. Non-Cryst. Solids*, 1988, **100**, 31; (e) H. Schmidt, *J. Non-Cryst. Solids*, 1988, **100**, 51; (f) C. Sanchez, J. Livage, M. Henry and F. Babonneau, *J. Non-Cryst. Solids*, 1988, **100**, 165; (g) U. Schubert, *J. Chem. Soc., Dalton Trans.*, 1996, 3343; (h) U. Schubert, H. Hüsing and A. Lorenz, *Chem. Mater.*, 1995, **7**, 2010; (i) H. Schmidt, H. Scholze and A. Kaiser, *J. Non-Cryst. Solids*, 1982, **48**, 65.
- 6 K. Tanabe, *Solid Acid and Bases*, Academic Press, New York, 1970.
- 7 (a) O. B. Koper, I. Lagadic, A. Volodin and K. J. Klabunde, *Chem. Mater.*, 1997, **9**, 2468; (b) T. Iizuka, H. Hattori, O. Yasuhiro, J. Sohma and K. J. Tanabe, *J. Catal.*, 1971, **22**, 130.
- 8 (a) K. J. Tanabe, H. Hattori, T. Sumiyoshi, K. Tamaru and T. J. Kondo, *J. Catal.*, 1978, **53**, 1; (b) H. Niiyama and E. Echigoya, *Bull. Jpn. Pet. Inst.*, 1972, **14**, 83.
- 9 (a) M. E. Llanos, T. Lopez and R. Gomez, *Langmuir*, 1997, **13**, 974; (b) T. Lopez, R. Gomez, M. E. Llanos and E. López-Salinas, *Mater. Lett.*, 1999, **38**, 283; (c) T. Lopez, R. Gomez, M. E. Llanos, E. Garcia-Figueroa, J. Navarrete and E. López-Salinas, *Mater. Lett.*, 1999, **39**, 51.
- 10 (a) J. A. Lercher and H. J. Noller, *J. Catal.*, 1982, **79**, 152; (b) A. M. Youssef, L. B. Khalil and B. S. Girgis, *Appl. Catal.*, 1992, **1**, 1.
- 11 K. J. Tanabe, M. Misono, Y. Ono and H. Hattori, in *New Solid Acids and Bases: Their Catalytic Properties*, ed. B. Delmon and J. T. Yates, *Studies in Surface Science and Catalysis*, Vol. 51, Elsevier, New York, 1989.
- 12 (a) K. S. W. Sing, D. H. Everett, R. A. W. Haul, L. Moscou, R. A. Pierotti, J. Rouquerol and T. Siemieniewska, *Pure Appl. Chem.*, 1985, **57**, 603; (b) S. J. Gregg and K. S. W. Sing, *Adsorption, Surface Area and Porosity*, 2nd edn., Academic Press, London, 1982.
- 13 S. Lowell and J. E. Shields, *Powder Surface Area and Porosity*, 2nd edn., Chapman and Hall, London, 1984.
- 14 (a) A. J. Lecloux, J. Bronckart, F. Noville, C. Dodet, P. Marchot and J. P. Pirard, *Colloids Surf.*, 1986, **19**, 359; (b) R. K. Iler, *The Chemistry of Silica*, John Wiley and Sons, New York, 1979.
- 15 G. W. Scherer, D. M. Smith and D. Stein, *J. Non-Cryst. Solids*, 1995, **186**, 309.
- 16 K. W. Terry, PhD thesis, U. C. San Diego, 1993.